ACS OMEGA

Open Access

http://pubs.acs.org/journal/acsodf

Article

Engineering Exosomes to Specifically Target the Mitochondria of Brain Cells

Xin Yan,[‖] Xinqian Chen,[‖] Zhiying Shan,[*] and Lanrong Bi[*]

Cite This: *ACS Omega* 2023, 8, 48984−48993

Read Online

ACCESS | Metrics & More | Article Recommendations

ABSTRACT: Mitochondrial dysfunction is associated with various health conditions, including cardiovascular and neurodegenerative diseases. Mitochondrial-targeting therapy aims to restore or enhance mitochondrial function to treat or alleviate these conditions. Exosomes, small vesicles that cells secrete, containing a variety of biomolecules, are critical in cell-to-cell communication and have been studied as potential therapeutic agents. Exosome-based therapy has the potential to treat both cardiovascular and neurodegenerative diseases. Combining these two approaches involves using exosomes as carriers to transport mitochondrial-targeting agents to dysfunctional or damaged mitochondria within target cells. This article presents a new technique for engineering brain-derived exosomes that target mitochondria and has demonstrated promise in initial tests with primary neuron cells and healthy rats. This promising development represents a significant step forward in treating these debilitating conditions.

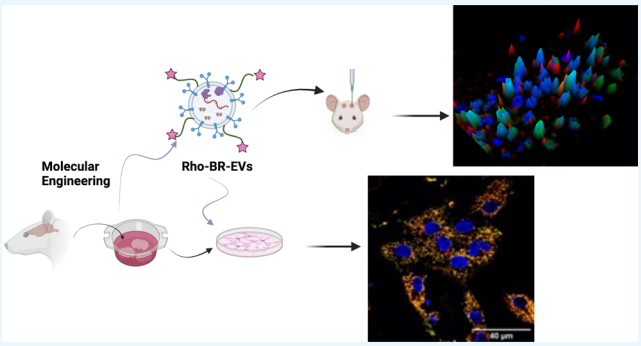

INTRODUCTION

Neurodegenerative diseases and cardiovascular diseases share several common risk factors,[1] such as hypertension, high cholesterol, diabetes, and obesity. These risk factors can lead to the development of vascular problems in the brain, which may increase the risk of neurodegenerative conditions such as Alzheimer's disease (AD) and vascular dementia. Additionally, chronic inflammation and oxidative stress associated with cardiovascular diseases have been linked to neurodegenerative diseases like Parkinson's disease (PD) and AD. Medications used to treat cardiovascular diseases may also have potential side effects on cognitive function, so it is essential to manage them effectively. Maintaining a heart-healthy lifestyle, including regular exercise and a balanced diet, and managing cardiovascular risk factors may also help reduce the risk of certain neurodegenerative diseases.

Brain damage represents a highly complex and multifaceted challenge for medical professionals. Conditions like brain tumors, stroke, and neurodegenerative disorders are complex to manage, with the blood−brain barrier (BBB) acting as a formidable obstacle that can hinder targeted treatment of affected areas in the brain.[2] The BBB can make it challenging to target diseased cells, which can impede treatment efficacy.[2] This challenge is particularly evident in the case of brain tumors, which can be highly invasive and difficult to remove.[3] Early diagnosis of neurodegenerative diseases can also be problematic, leading to limited treatment options and reduced chances of successful intervention.[4] Despite the challenges, there is hope for the future. Researchers are constantly exploring new ways to overcome the BBB, target diseased cells, and enhance therapeutic efficacy to unlock new treatment possibilities and improve patient outcomes.

As the field of cardiovascular and neurodegenerative diseases progresses, one promising area of focus is targeting mitochondria. These powerhouses of the cell are responsible for producing energy and regulating cellular metabolism, making them crucial components of overall cellular health. Dysfunctional mitochondria have been linked to various diseases, including myocardial infarction, hypertension, AD,[5] PD,[5] and brain tumors.[6] There are several reasons why targeting mitochondria may be beneficial in treating these conditions.[7,8] For instance, enhancing ATP production can help restore energy balance within cells, which is often disrupted in neurodegenerative diseases.[9] Additionally, reducing reactive oxygen species (ROS) production can protect cells from oxidative damage, which is thought to contribute to the development and progression of many diseases. Targeting mitochondria may also help regulate apoptosis (programmed

Received: September 2, 2023
Revised: November 22, 2023
Accepted: November 24, 2023
Published: December 11, 2023

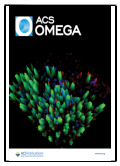

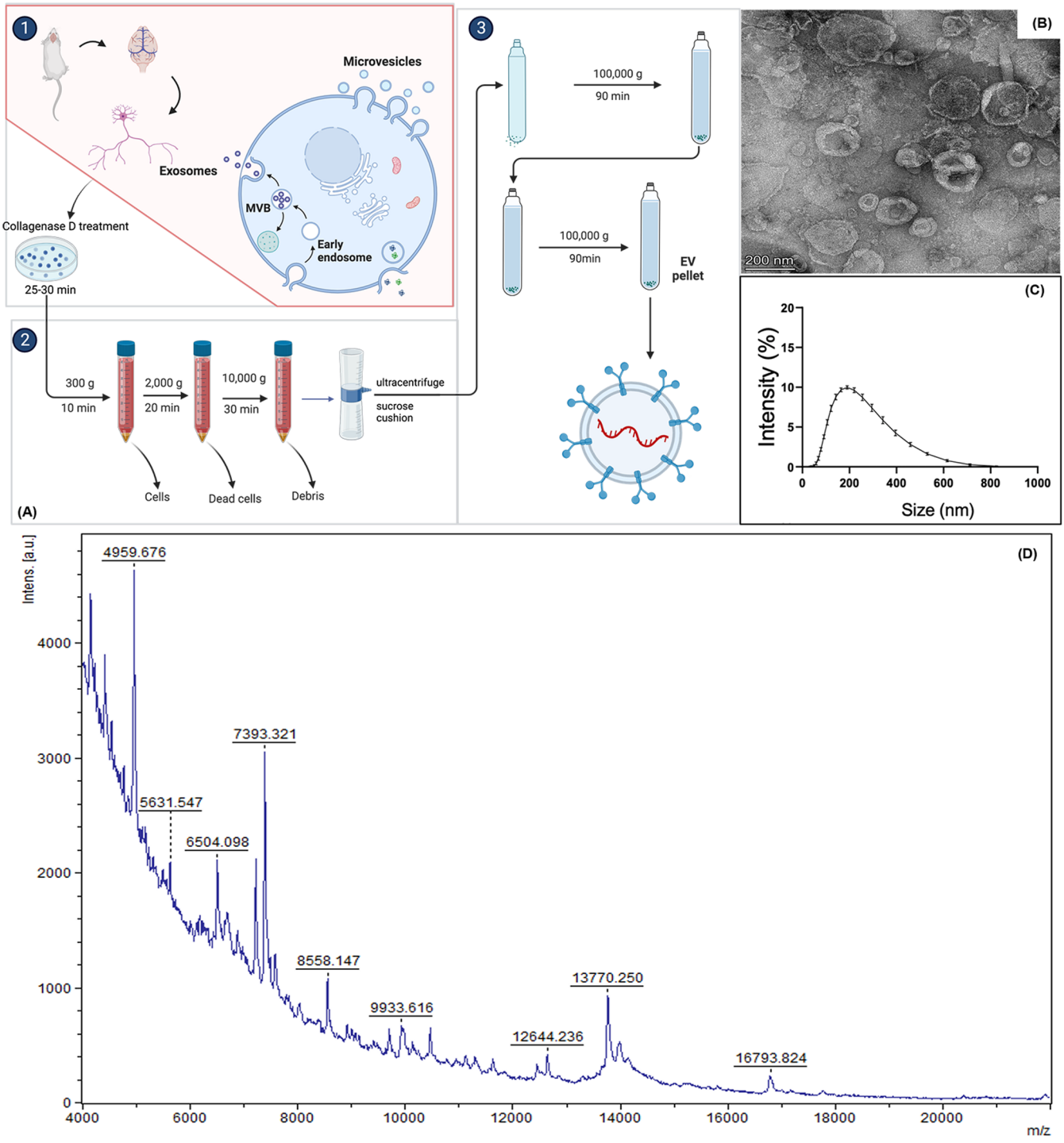

Figure 1. Preparation and characterization of the brain-derived exosomes, BR-EVs. (A) Preparation of modified exosomes (Rho-EVs) by ultracentrifugation. (B) TEM image of BR-EVs. (C) DLS analysis of BR-EVs. (D) The molecular content of BR-EVs was analyzed by MALDI-TOF mass spectrometry.

cell death), which can be dysregulated in cancer cells.[10] Protecting neurons from damage is another potential benefit of such therapies, as is repairing mitochondrial DNA mutations that can contribute to disease development. Furthermore, targeting mitochondria can enable more precise and efficient drug delivery, improving treatment outcomes and reducing side effects. While these potential benefits are promising, further research is necessary to develop effective, safe, and mitochondrial-targeted therapies.

In recent years, exosomes have been gaining attention as a promising option for drug delivery.[11−13] These small extracellular vesicles can naturally cross the BBB, allowing targeted treatments for neurological conditions. BR-EVs are biocompatible and exhibit low immunogenicity, making them an ideal choice for drug delivery applications. These features make BR-EVs an attractive therapeutic option for treating brain diseases. Our research team has hypothesized that by modifying the composition of the exosomal membrane, we can

https://doi.org/10.1021/acsomega.3c06617
ACS Omega 2023, 8, 48984−48993

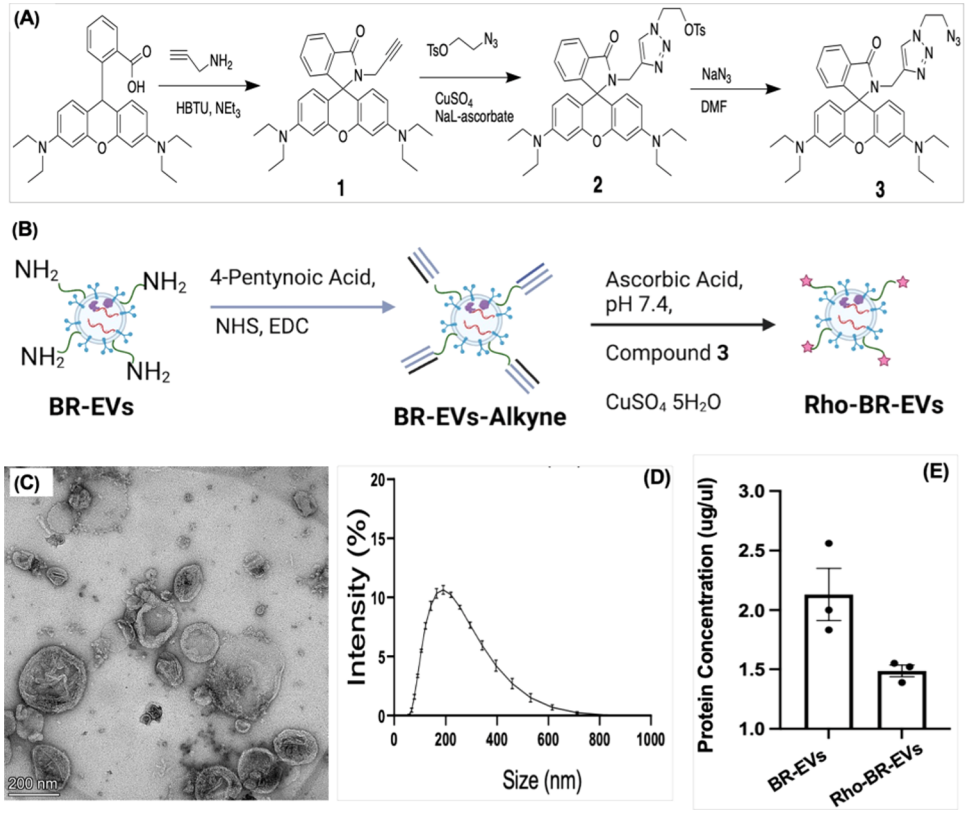

Figure 2. Preparation and characterization of MTEs (Rho-BR-EVs) based on brain-derived exosomes. (A) Preparation of a mitochondrial-targeting ligand (MTL), i.e., rhodamine-derived 3. (B) Chemical modification of exosomal surface proteins using a copper(I)-catalyzed azide−alkyne cycloaddition (CuAAC). (C) TEM image of Rho-BR-EVs. (D) DLS analysis of Rho-BR-EVs. (E) Protein content analysis of Rho-BR-EVs and unmodified BR-EVs.

enhance targeting and improve drug loading efficiency, which could ultimately lead to more effective treatments for brain diseases. This article presents our findings on preparing and characterizing BR-EVs with mitochondria-targeting capabilities, which could be a potential therapeutic strategy for brain damage caused by cardiovascular and neurodegenerative diseases.

RESULTS AND DISCUSSION

Preparing BR-EVs from rat brains is a complex process that involves several steps (Figure 1A). First, the rats are euthanized with an overdose of isoflurane, and their brains are carefully removed and cut into small pieces. The exosomes are then separated from other cellular components using ultracentrifugation. Finally, various techniques such as transmission electron microscopy (TEM), dynamic light scattering (DLS), and matrix-assisted laser desorption/ionization time-of-flight (MALDI-TOF) mass spectrometry are employed to confirm the identity of the isolated exosomes.

The size of unmodified and modified BR-EVs can affect their cellular uptake, stability, and functional properties, making investigations of their size distribution crucial. DLS is a relatively quick and nondestructive technique, making it suitable for measuring exosomes in their native state. It measures the fluctuations in dispersed light intensity resulting from the Brownian motion of particles in solution.[12]

As shown in Figure 1C, the hydrodynamic sizes of BR-EVs are approximately 120−200 nm. It is important to remember that the hydrodynamic sizes of exosomes measured by DLS include the size of the exosome itself, the surrounding water molecules, and any solutes or biomolecules present in the suspension. This means that the measured size may not reflect the actual size of the exosome core alone. DLS provides information about the size distribution of the exosomes in a sample. Therefore, additional complementary techniques, such as TEM, are often used with DLS to better understand the characteristics of exosomes' characteristics better.

As shown in Figure 1C, BR-EVs typically range in size from approximately 30 to 150 nm. BR-EVs generally have a cup-shaped or saucer-like morphology formed by the inward budding of the endosomal membrane (Figure 1B). The characteristics of BR-EVs may vary in different biological contexts due to various factors such as cell type, cellular state, and environmental conditions.[13]

MALDI-TOF mass spectrometry is a powerful tool for exosome characterization and has contributed to our understanding of exosome biology and its potential diagnostic and therapeutic applications.[14] As shown in Figure 1D, the obtained mass spectra correspond to the proteins and other biomolecules present in the exosomes. Currently, we are analyzing the mass spectra and hope to gain insights into the protein composition and heterogeneity of exosomes, identify potential biomarkers, and compare exosomal content from different sources or disease states to gain insights into the functional roles of exosomes in physiological and pathological processes.

BR-EVs comprise a lipid bilayer membrane encapsulating various molecules, including proteins, nucleic acids, lipids, and metabolites.[11] These molecules include some proteins with amino groups on the exosomal surface, which can be modified

https://doi.org/10.1021/acsomega.3c06617
ACS Omega 2023, 8, 48984−48993

chemically for various purposes. By chemical modification of the BR-EVs, we can enhance their functionality and customize them for specific applications. The modifications can be used to attach diagnostics or therapeutic agents to the exosomal surface, which allows for better targeting specificity, enables targeted delivery to specific organelles, and facilitates the visualization and tracking of exosomes in brain mitochondria.

To improve their targeting specificity and therapeutic potential, we modified the amino groups on the surfaces of exosomes. More specifically, 4-pentynoic acid, *N*-hydroxysuccinimide (NHS), and 1-ethyl-3-(3-(dimethylamino)propyl) carbodiimide (EDC) were used to introduce alkyne functionality to the surface of BR-EVs. The process involves activating the carboxylic acid groups on the BR-EVs' surface with NHS and EDC and then adding activated 4-pentynoic acid to the solution to form stable amide bonds with primary amines on the BR-EVs' surface. This results in covalently attached alkyne groups on the surface of BR-EVs, which can be used for subsequent bioconjugation reactions. This approach allows modifications or specific interactions with other molecules through a "click" chemistry. We utilized the alkyne functionality as a site for chemical conjugations with a mitochondrial-targeting ligand (MTL), rhodamine derivative **3** (Figure 2A), via a "click" chemistry based on copper(I)-catalyzed azide−alkyne cycloaddition (CuAAC).[15,16] Rhodamine derivatives have a unique structure with a central xanthene ring system that can be modified to add specific properties or targeting capabilities.

Some rhodamine derivatives have been created to target specific organelles for selective accumulation.[17−20] This makes them valuable tools for studying mitochondrial function and dynamics. Finally, we isolated and purified the modified exosomes, Rho-BR-EVs, by using a Sepharose CL-4B column. This versatile method of modifying exosomes using CuAAC has allowed us to create a new diagnostic and therapeutic tool.

Upon conducting thorough TEM and DLS analyses before and after the chemical modification process, we found that the resulting modifications have not significantly impacted the exosome morphology (Figure 2C) and size (Figure 2D). This leads us to confidently conclude that the chemical modification process is safe for use because of its effects on the physical characteristics of the exosomes. However, it is worth noting that these analyses only provide information on the size and morphology of the exosomes. While these physical characteristics are certainly important, other aspects of exosomes may require further evaluation using additional methods.

When working with modified exosomes, it is important to examine their proteins to fully understand the changes that occur during the modification process and evaluate their safety and efficacy for different applications. Through our analysis using the Bradford protein assay, we observed some extent of protein loss (Figure 2E), which is normal during the isolation and purification. However, this may pose a problem during the modification and purification. Optimizing the protocols and procedures and implementing quality control measures to ensure the accurate characterization of modified exosomes are crucial to minimizing protein loss.

Next, we examined the subcellular localization of modified exosomes by preparing and cultivating primary neuron cells. To achieve this, we isolated primary neurons from the brains of neonatal Sprague−Dawley (SD) rats. We cultured them in specialized neuronal culture media under controlled incubator conditions until they had matured. Upon maturity, we introduced Rho-BR-EVs into the culture media and allowed the cells to take up these modified exosomes.

We obtained high-resolution images of cells by using confocal microscopy to investigate subcellular localization further. We counterstained the cultures with MitoTracker, a fluorescent mitochondria-specific marker, to enhance visualization. Upon merging the confocal images of Rho-BR-EVs and MitoTracker, we successfully observed colocalization with the MitoTracker, which indicated that the modified exosomes had targeted the intended subcellular location. To gain insights into the behavior of Rho-BR-EVs in cells, we conducted a time course study over 72 h, closely monitoring changes in fluorescence intensity and localization (Figure 3). It appears

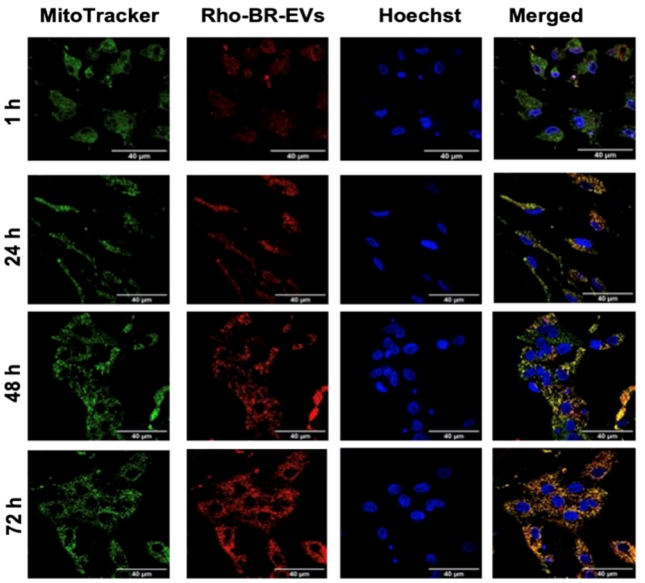

Figure 3. Representative confocal fluorescence pictures of primary neurons incubated with Rho-BR-EVs (2 g/mL, red fluorescence), MitoTracker (80 nM, green fluorescence), Hoechst 33242 (0.1 g/mL, blue), and merged images (yellow). The Rho-BR-EV time course investigation was conducted at various time points (1, 24, 48, and 72 h). The fluorescence pictures were captured using a confocal laser scanning fluorescence microscope with a 60× objective lens and medium free of FBS and phenol-red.

that the uptake of Rho-BR-EVs in primary neuron cells is dependent on time, and the fluorescence intensity increases over time. This finding suggests that the level of uptake of exosomes increases over an extended time. Exosomes are important for cell communication, as they can transfer various molecules, such as proteins, nucleic acids, and lipids. In our present study, the fluorescence intensity of Rho-BR-EVs increased with time, indicating an accumulation of these modified exosomes within the cells or an increasing uptake rate as time progressed. Upon the analysis of these results, we hypothesize that endocytosis was likely the cells' primary method of Rho-BR-EV uptake. Once internalized through endocytosis, the Rho-BR-EVs must be able to escape the endosomal compartment and target the mitochondria, as shown in Figure 4.

Brain damage caused by AD can have a significant impact on two key regions of the brain, namely, the hippocampus and the cortex. These regions are responsible for higher cognitive functions, such as memory formation, spatial navigation, language, attention, and executive functions. Unfortunately,

https://doi.org/10.1021/acsomega.3c06617
ACS Omega 2023, 8, 48984−48993

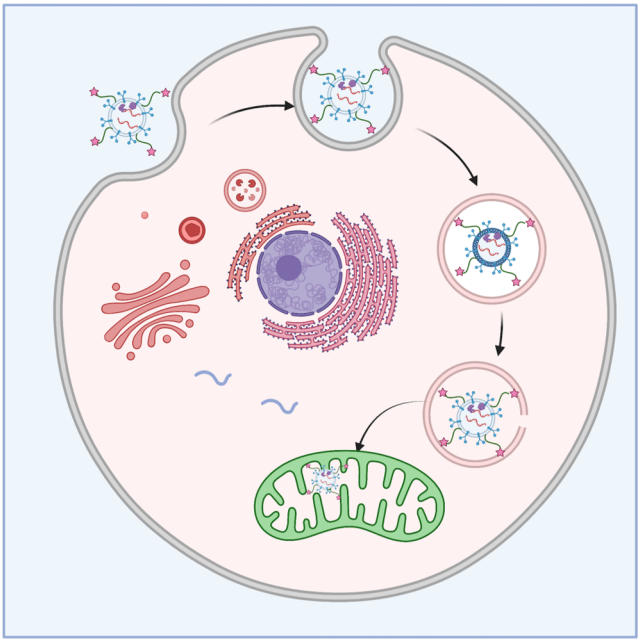

Figure 4. It is assumed that cells use endocytosis to absorb Rho-BR-EVs. After entering the cell, the Rho-BR-EVs must break free from the endosomal compartment and target the mitochondria. Rho-BR-EVs tend to group in a specific manner within the mitochondria, likely due to the unique properties of the rhodamine derivative, which can pass through the mitochondrial membrane and is attracted to the negative charge on the inner membrane, resulting in the characteristic punctate pattern of Rho-BR-EVs within the mitochondria.

AD can disrupt these functions and cause impairments. Therefore, we conducted a thorough study of the uptake and distribution of Rho-BR-EVs in these regions.

Rho-BR-EVs were delivered into rat brains through intracerebroventricular (ICV) injection. 24 h after the ICV injection, rats were euthanized, their brains were sectioned, and the distribution of Rho-BR-EVs was observed. Our findings showed that Rho-BR-EVs were present in the hippocampus (Figure 5) and cortex (Figure 6), indicating that cells like neurons and glial cells had absorbed them.

NeuN is a commonly used marker for detecting and labeling neurons. It binds to the neuronal cell nuclei and helps distinguish neurons from other types of cells in the nervous system and brain. NeuN labeling primarily identifies and labels neurons in tissue sections or cultures. We applied NeuN antibodies to the samples, which specifically bind to NeuN proteins in the neurons' nuclei. Therefore, colocalization of NeuN with mitochondrial-targeted Rho-BR-EVs is not expected. Observations indicate that Rho-BR-EVs accumulate around neuron cells, suggesting that neurons may interact with or take up these engineered exosomes. Neurons are known to take up exosomes, which can transfer signaling molecules or genetic material and play a role in the maintenance and function of neurons. Further experiments or studies are required to confirm that neuron cells are taking up the engineered exosomes. The internalization process needs to be more closely monitored, and functional assays or molecular analysis will help to determine the effects and mechanisms of engineered exosome uptake by neuron cells.

GFAP is a type of protein mainly present in astrocytes, a specific type of glial cell that is found in the central nervous system. We used GFAP labeling to identify and visualize astrocytes in these experiments. In our present study, we found that Rho-BR-EVs, engineered exosomes, accumulate around astrocytes labeled with GFAP. This observation suggests that these exosomes are in close proximity to astrocytes and may be interacting with them. However, it is essential to note that this accumulation does not definitively prove that astrocytes take up the Rho-BR-EVs. To confirm the interaction, further investigation is necessary. Nonetheless, the accumulation of Rho-BR-EVs around GFAP-labeled astrocytes is a promising finding that requires further exploration.

Rho-BR-EVs are also observed to accumulate around IBA1-labeled microglia, indicating a possible interaction or association between the two. Rho-BR-EVs do not colocalize with the microglia despite accumulation, suggesting that they may not be present within the same cellular compartment. It is possible that Rho-BR-EVs are internalized by the microglia but may not have fully merged with the microglial cellular contents, or they may be being taken up. This dynamic interaction between the engineered exosomes and microglia requires further investigation to understand the precise mechanisms of uptake and the functional consequences of this interaction.

We have observed that the Rho-BR-EVs gather around neuron, microglial, and astrocyte cells in the hippocampus (Figure 5) and cortex (Figure 6), indicating that they may interact and home in on these cells. This observation could have important implications for intercellular communication and crosstalk. It may suggest that the engineered exosomes could be either maintaining or enhancing the ability of these cells to communicate with each other, which is particularly critical in the central nervous system, where complex signaling and crosstalk between neurons, microglia, and astrocytes is necessary to maintain brain function and respond to various stimuli.

To assess the possibility of any neuroinflammation in rats caused by the injection of Rho-BR-EVs, we measured the levels of GFAP (Figures 5B and 6B) and IBA1 fluorescence intensity (Figures 5C and 6C). The results showed that there were no significant changes in the IBA1 and GFAP fluorescence intensity in the rats receiving Rho-BR-EVs compared with the sham-control group. Inflammatory markers such as IBA1 and GFAP are often used to assess neuroinflammation. The absence of significant changes in their fluorescence intensity suggests that the injection of Rho-BR-EVs did not cause any detectable neuroinflammation in the rats. IBA1 is a marker for activated microglia, and GFAP is for astrocytes. The activation of these cells can often be linked to neuroinflammatory processes. Nonetheless, the lack of significant changes in their fluorescence intensity indicates that the Rho-BR-EVs did not trigger an inflammatory response in the rat brain. While the absence of detectable neuroinflammation is promising, further research is required to fully understand the effects of Rho-BR-EVs in other contexts and potential long-term effects.

CONCLUSIONS

We have developed a new method for preparing exosomes that can specifically target mitochondria and tested this approach both in vitro and in vivo. This exciting breakthrough has significant potential for improving targeted drug delivery by enabling us to deliver drugs directly to specific tissues, cells, and organelles within the body. Furthermore, our discovery of Rho-BR-EVs within mitochondria could have far-reaching

https://doi.org/10.1021/acsomega.3c06617
ACS Omega 2023, 8, 48984−48993

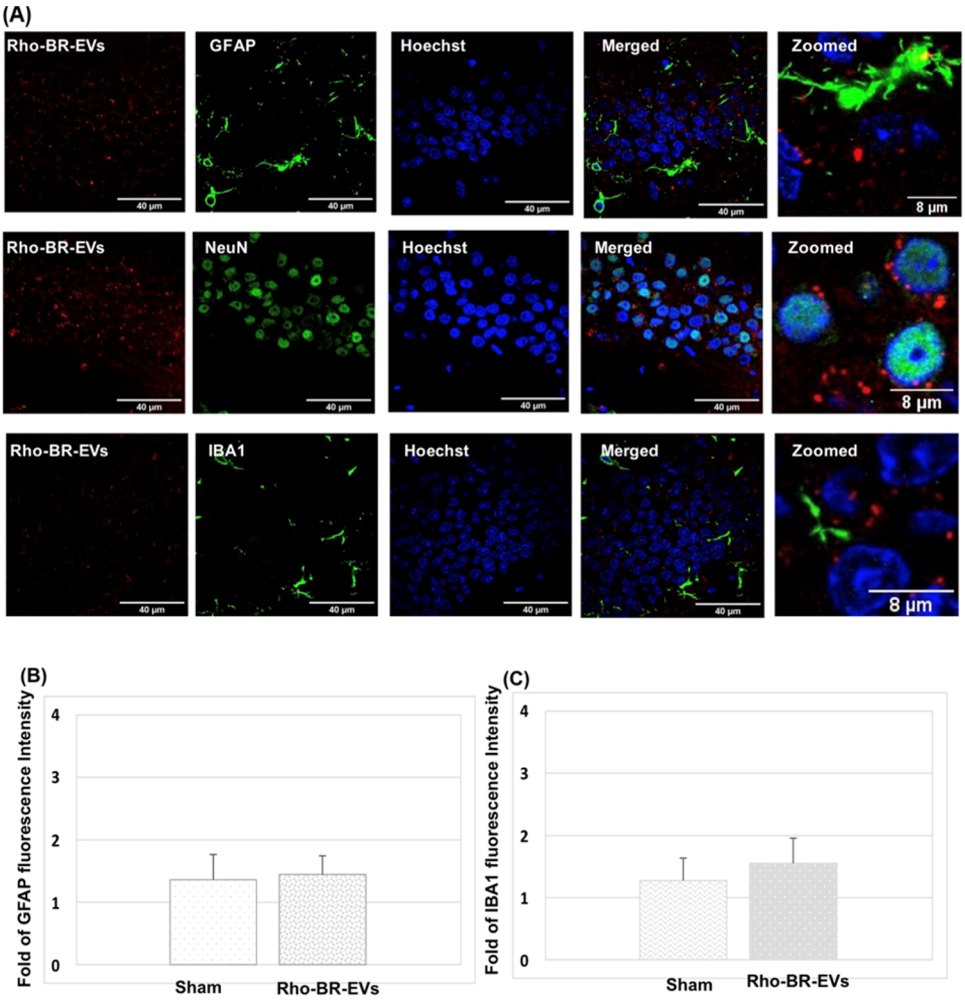

Figure 5. Rho-BR-EV visualization in hippocampal regions: (A) Images of confocal laser scanning of rat brain slices fixed with 4% PFA. The red channels indicate fluorescently labeled exosomes (Rho-BR-EVs) throughout the picture. In contrast, the green channels reflect GFAP-positive (row I), NeuN-positive (row II), and IBA1-positive (row III) cells in brain slices. On the right, zoomed-in images are exhibited. The fluorescence images were captured using a 60× objective lens on a confocal laser scanning fluorescence microscope. (B) Mean fluorescence intensity of GFAP and (C) IBA1 label in hippocampal regions. *Z*-section thickness is estimated to be 0.0083 μm/slice.

implications for studying mitochondrial function or dysfunction.

Our research has successfully demonstrated the subcellular localization of engineered exosomes in primary neuron cells, highlighting the immense potential of these engineered exosomes for targeted drug delivery. This approach could revolutionize the field of drug delivery, enabling the targeted delivery of drugs to specific subcellular locations, thereby enhancing therapeutic efficacy and minimizing adverse effects.

■ LIMITATIONS

Determining the targeting specificity and fluorescence intensity of engineered exosomes in brain tissues can be challenging due to the complexity of brain tissue and the high autofluorescence of brain regions. To address this issue, Rho-BR-EVs were directly administered into the cerebrospinal fluid (CSF) within the brain's ventricles using ICV injection. Our initial data revealed that Rho-BR-EVs could travel through the CSF circulation and be taken up by various cells in different brain regions, indicating their potential to deliver drugs to the brain. However, it is essential to note that ICV injection is an invasive procedure that requires specialized equipment and skills for safe execution and may pose risks of infection, inflammation, and damage to brain tissue.

We recently discovered that Rho-BR-EVs could cross the BBB through peripheral administration, such as intravenous or intraperitoneal injection (data not shown). This new drug delivery system to the central nervous system shows promise and is safe for the treatment of brain diseases.

Translating research findings from animal models to potential clinical trials is complex, involving conducting preclinical studies on animals. The next goal of our studies is to determine the safety profile, dosage, and therapeutic potential of brain-derived exosomes that target mitochondria. This process involves checking for potential adverse effects and determining the most effective delivery methods. Since rats and humans have significant biological differences, what works in a rat model may not work the same in humans due to physiological, metabolism, and immune system variations. Therefore, for the exosomes to effectively target mitochondria in human cells, it is necessary to verify their specificity and efficiency of mitochondria targeting in the relevant human cell types. Additionally, further toxicology and pharmacokinetic studies are required.

https://doi.org/10.1021/acsomega.3c06617
ACS Omega 2023, 8, 48984−48993

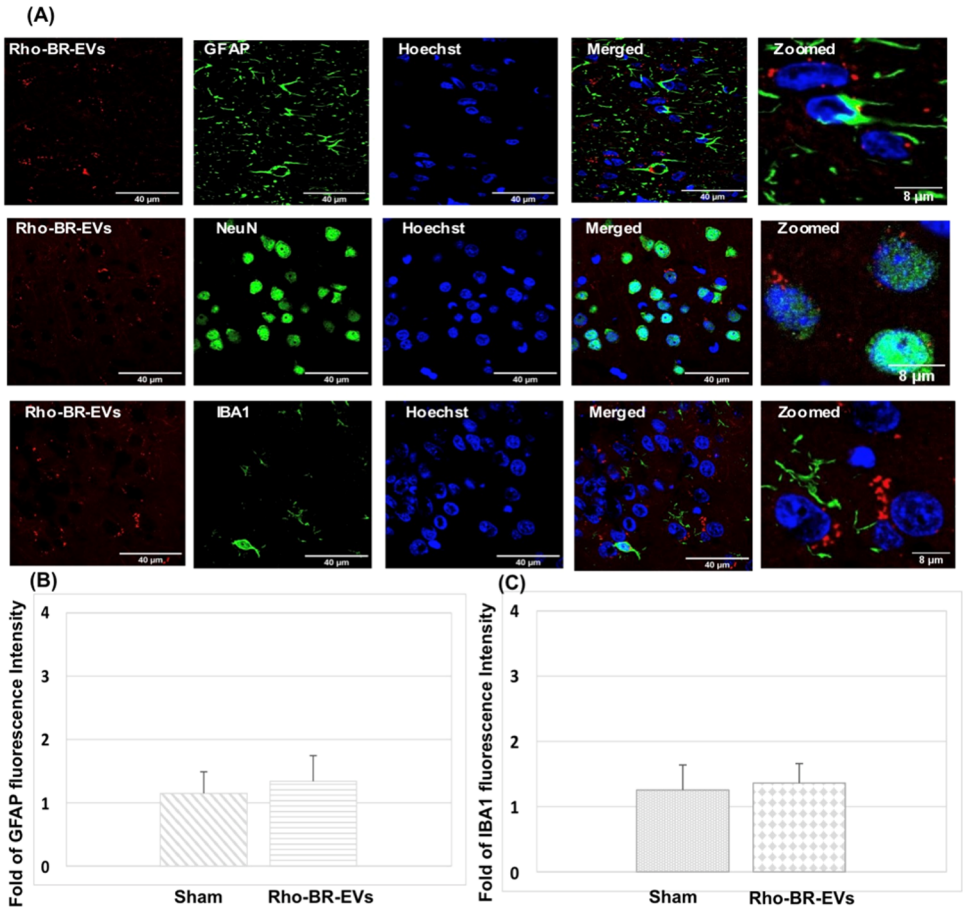

Figure 6. Rho-BR-EV visualization in cortical regions: (A) Images of confocal laser scanning of rat brain slices were fixed with 4% PFA. The red channels indicate fluorescently labeled exosomes (Rho-BR-EVs) throughout the figure. In contrast, the green channels reflect GFAP-positive (row I), NeuN-positive (row II), and IBA1-positive (row III) cells in brain slices. On the right, zoomed-in images are exhibited. The fluorescence pictures were captured using a 60× objective confocal laser scanning fluorescence microscope. (B) Mean fluorescence intensity of GFAP and (C) IBA1 label in hippocampal regions. *Z*-section thickness is estimated to be 0.0083 μm/slice.

MATERIALS AND METHODS

Procedure for Synthesizing Compound 1.[21] In 20 mL of anhydrous dichloromethane, 0.90 g (1.80 mmol) of rhodamine B was dissolved. Propargylamine (0.12 mL, 2.0 mmol), 2-(1*H*-benzotriazol-1-yl)-1,3,3-tetramethyluronium-hexafluorophosphate (HBTU, 0.783 g, 2.0 mmol), and triethylamine (1 mL, 5.76 mmol) were added to the mixture. The mixture was stirred at room temperature overnight. The mixture was rinsed three times with brine after being diluted with 20 mL of dichloromethane. The organic layer was then vacuum-evaporated, filtered, and dried over anhydrous sodium sulfate. The final product was purified by flash column chromatography on silica gel (hexane/EtOAc, 4:1) to produce compound **1** (0.86 g, 80%) as a light pink solid. ^{1}H NMR (400 MHz, $CDCl_3$) δ ppm 1.14 (t, J = 7.2 Hz, 12 H), 1.74 (t, J = 2.4 Hz, 1H), 3.32 (q, J = 7.2 Hz, 8H), 3.93 (d, J = 2.4 Hz, 2H), 6.25 (dd, J = 8.8, 2.8 Hz 2H), 6.37 (d, J = 2.8 Hz, 2H), 6.45 (d, J = 8.8 Hz, 2H), 7.10 (m, 1H), 7.41 (m, 2H), 7.91 (m, 1H). ^{13}C NMR (101 MHz, $CDCl_3$) δ: 189.81, 167.47, 153.89, 153.61, 148.99, 132.78, 130.60, 129.27, 128.16, 123.95, 123.18, 108.22, 105.33, 98.03, 78.54, 70.27, 65.04, 44.68, 28.84, 12.91.

Synthetic Procedure for Compound 2.[21] To a stirring solution of compound 1 (0.5 g, 1.00 mmol) and 2-azidoethyl 4-methylbenzene-sulfonate (0.45 g, 1.25 mmol) in THF/*tert*-butanol/water = 3:1:1, copper(II) sulfate (0.21 mmol, 40 mg) and sodium ascorbate (0.42 mmol, 82 mg) were subsequently added. After that, the reaction mixture was stirred at room temperature for 6 h. The reaction was rinsed with 10 mL of saturated $NaHCO_3$ 3 times before extracting 40 mL of ethyl acetate. The organic layers were mixed, dried over anhydrous sodium sulfate, filtered, and concentrated. The crude residue was purified by flash column chromatography on silica gel (eluent: hexane/EtOAc = 1:4) to obtain compound **2** (0.62 g, 80%) as colorless foam.^{1}H NMR (400 MHz, $CDCl_3$) δ ppm 1.09 (t, J = 7.0 Hz, 12H), 2.32 (s, 3H), 3.26 (q, J = 7.0 Hz, 8H), 4.21 (t, J = 5.0 Hz, 2H), 4.29 (t, J = 5.0 Hz, 2H), 4.37 (s, 1H), 6.12 (dd, J = 8.8, 2.0 Hz, 2H), 6.24 (d, J = 8.8 Hz, 2H), 6.31 (d, J = 2.0 Hz, 2H), 6.84 (s, 1H), 7.10−6.94 (m, 1H), 7.21 (d, J = 8.5 Hz, 2H), 7.47−7.29 (m, 2H), 7.65−7.46 (m, 2H), 8.09−7.73 (m, 1H). ^{13}C NMR (100 MHz, $CDCl_3$) δ ppm: 168.03, 153.04, 153.61, 148.95, 145.64, 144.76, 132.79, 132.23, 131.19, 130.26, 129.03, 128.32, 127.98, 124.14, 123.40, 123.09, 108.13, 105.50, 98.01, 76.92, 67.48. 65.19, 48.60, 44.53, 35.58, 21.84, 12.81.

Synthetic Procedure for Compound 3.[21] NaN_3 (70 mg, 1.00 mmol) was added to a solution of compound **2** (0.50 g, 0.70 mmol) in 10 mL of DMF while stirring. Overnight, the reaction mixture was gently refluxed. The reaction mixture was rinsed 3 times with 10 mL of saturated $NaHCO_3$ and extracted with 40 mL of EtOAc. The organic layers were combined, desiccated over anhydrous Na_2SO_4, filtered, and evaporated in

https://doi.org/10.1021/acsomega.3c06617
ACS Omega 2023, 8, 48984−48993

vacuum. Compound **3** (0.40 g, 96%) was obtained as a white froth after the crude residue was purified by flash column chromatography on silica gel (eluent: hexane/EtOAc = 1:3).^{1}H NMR (400 MHz, $CDCl_3$) δ ppm 1.14 (t, J = 7.2 Hz, 12H), 3.30 (q, J = 7.2 Hz, 8H), 3.60 (t, J = 6.1 Hz, 2H), 4.20 (t, J = 6.1 Hz, 2H), 4.47 (s, 2H), 6.15 (dd, J = 8.9, 2.5 Hz, 2H), 6.30−6.33 (m, 4H), 6.95−7.18 (m, 3H), 7.37 (m, 2H), 7.86 (m, 1H). ^{13}C NMR (101 MHz, $CDCl_3$) δ: 167.94, 153.56, 153.54, 148.82, 144.68, 132.71, 131.08, 128.96, 128.24, 124.03, 123.19, 123.02, 108.00, 105.54, 98.02, 65.25, 60.60, 50.68, 49.00, 44.60, 35.54, 19.48, 14.53, 12.94.

■ ANIMALS

Adult SD rats used in this study were purchased from Charles River Laboratories (Wilmington, MA). All animals were obtained on a 12/12 h light/dark cycle in a climate-controlled room, and the chow and water were provided ad libitum. This study was carried out in strict accordance with the recommendations in the Guide for the Care and Use of Laboratory Animals of the National Institutes of Health. The Michigan Technological University Institutional Animal Care and Use Committee approved the protocol.[22]

Preparation of Brain-Derived Exosomes (BR-EVs). Extracellular vesicles (EVs) were isolated based on established protocols with some modifications.[23,24] Fresh rat brains (whole brains without the cerebellum) preserved in phosphate-buffered saline (PBS) were cut into minute pieces on ice. Following the transfer, tissue fragments weighing 200 mg were placed in a 6-well plate containing 2 mL of Hibernate E (Gibco) in each well. They were carefully dissociated until all of the pieces were the same size: approximately 2 mm on one side, 2 mm on the length, and 2 mm on the height. Subsequently, 40 μL of Collagenase D (Sigma-Aldrich) and 4 μL of DNase I (Sigma-Aldrich) were added to each well to reach a final concentration of 2 mg/mL for Collagenase D and 40 U/mL for DNase I. The plate was immediately transferred into a prewarmed 37 °C incubator under mild agitation (70 rpm) for 30 min. Immediately following the incubation step, the plate was placed back on the ice, and protease and phosphatase inhibitors (Sigma-Aldrich) were added to each well. Tissue fragments containing Hibernate E were drained into a 50 mL tube by gravity through a 70 μm sterile cell strainer. An additional 1−2 mL of PBS was added to each well to transfer the remaining tissue fragments. Differential centrifugation was performed on the following filtered samples: (I) 300g, 10 min, 4 °C; (II) 2000g, 20 min, 4 °C; and (III) 10,000g, 30 min, 4 °C. To remove larger particulates from the sample, the supernatants were collected and filtered through a 0.22 μm filter (Grainger Industrial Supply). The filtered supernatants were progressively layered over 4 mL of a 30% sucrose solution prepared in PBS before being centrifuged at 100,000g for 90 min at a temperature of 4 °C (Optima XL-90 ultracentrifuge, SW 28 centrifuge rotor, Beckmann-Coulter). The supernatant was discarded, and the sucrose layer (approximately 5 mL) and pellets were collected. Additional ultracentrifugation (100,000g, 90 min, 4 °C) was performed, and the pellets were resuspended in 50 μL of ice-cold PBS for subsequent steps. Total BR-EV proteins were extracted with a RIPA buffer containing 0.5% PMSF (Sigma-Aldrich). In brief, BR-EVs were subjected to an equal volume of supplemented RIPA buffer and sonicated 3 times with each 5 s interval. Sonicated BR-EV samples were lysed on ice for 20 min and mixed with pipetting every 5 min. Protein quantification was determined with Bradford reagent (Sigma-Aldrich).

Preparation and Culture of Primary Neuron Cells. In neuroscience research, primary neuron cells derived from postnatal rat brains are extensively used as an in vitro model to explore neuronal development, function, and neurological disorders.[22,25]

Neurons were isolated from the brains of 1-day-old SD pups using a papain dissociation system (Worthington Biochemical Co.) following the manufacturer's instruction. First, SD pups were euthanized using an overdose of isoflurane, and their whole brains were removed and placed in a sterile culture dish containing cold PBS. The blood vessels and meninges surrounding the brain were removed, and the cerebellum and brainstem were removed. The remaining brain region containing the neurons of interest (e.g., hippocampus and cortex) was transferred to a new culture dish and cut into small (1−2 mm) pieces. In a sterile tube containing prewarmed papain solution, the tissue pieces were placed and incubated at 37 °C with constant agitation for 60 min.

After this enzymatic reaction, the mixture was gently triturated using a sterile Pasteur pipet to release cells. The cloudy cell suspension was centrifuged to collect cells. The cells were further purified with discontinuous density gradient centrifugation, as detailed in the manufacturer's manual. Cell concentration was then determined by using cell counting equipment. The cell suspension was then diluted with neurobasal media supplemented with B27 serum to reach the desired cell density. The cells were then plated onto poly-D-lysine-coated culture dishes at the appropriate cell densities and volumes, incubated in a 5% CO_2 incubator for 7−10 days, and ready for the experiment. Half of the culture medium was replaced with fresh medium every 3 days. The cells' growth and well-being were monitored regularly using a microscope.

Modification of Exosomes' Surface Using NHS Ester Chemistry. *Alkyne-Modified Exosomes.* After adding 290 mg of propargylacetic acid (3 mmol) and 350 mg of n-hydroxysuccinimide (3 mmol) to 10 mL of PBS with stirring, the resulting solution was adjusted to pH 7.4 with sodium bicarbonate. After 1 h of stirring in an ice bath, 460 mg of 1-ethyl-3-(3-carbodiimide dimethyl aminopropyl) was added, followed by another hour of stirring in an ice bath. Then, 100 μL of the reaction mixture was added to 250 μL of the exosome solutions, followed by 24 h of shaking at room temperature. Exosomes were isolated from the excess reaction material using a pH 7.4 PBS-conditioned Sepharose CL-4B column.

Preparation of Rho-BR-EVs via a "Click" Chemistry Based on Copper(I)-Catalyzed Azide−Alkyne Cycloaddition (CuAAC). Labeling alkyne-modified exosomes with azido-rhodamine (compound **3**) was a two-step process. First, the exosomes were labeled with compound **3** via a copper-catalyzed "click" chemistry reaction, and then, the labeled exosomes were purified to remove any unbound dye and excess reactants.

The alkyne-modified exosomes were thawed and diluted to a final concentration of 1−2 mg/mL in PBS buffer. In a microcentrifuge tube, the components were combined to make the copper-catalyzed click chemistry reaction mixture: azido-rhodamine (compound **3**), 10−20 μg/mL of exosome solution; copper sulfate, 50 μM; sodium ascorbate, 100 μM; TCEP, 1 mM; DMSO, 10% final concentration. Briefly, the reaction mixture was agitated and then added to the exosome

https://doi.org/10.1021/acsomega.3c06617
ACS Omega 2023, 8, 48984−48993

solution while stirring gently. The mixture was protected from light and incubated at room temperature for 1−2 h. After incubation, 10−15 mL of PBS buffer was added to the reaction mixture and transferred to an ultracentrifuge tube. To extract Rho-BR-EVs, the reaction mixture was centrifuged at 100,000*g* for 1 h at 4 °C. The exosome particle was resuspended in 1 mL of PBS buffer, and the supernatant was discarded. The ultracentrifugation step was repeated to remove the unbound dye and superfluous reactants from the exosomes, which were then washed. The exosome particle was reconstituted in 50−100 μL of PBS buffer, and the supernatant was discarded.

Dynamic Light Scattering (DLS) Analysis of Exosomes. Light scattering in resuspended pellets was diluted with DPBS to achieve a final protein concentration of 0.01 μg/μL. Diluted samples were put into a low-volume cuvette, and the size distribution of exosomes was determined using the Malvern Zetasizer nano series. Cuvettes with lids were mixed upside down to avoid large particles from remaining at the bottom. In each sample, the measurement was repeated 3 times.

Morphology Analysis by TEM. 30 μL of resuspended exosomes were mixed with an equal volume of 2% paraformaldehyde (PFA) for 5 min. 5 μL of the specimen was loaded on the carbon side of the grid and left for 1 min. Subsequently, the sample was gently blotted dry with clean filter paper. Negative staining was performed with uranyl acetate (UA). A 3 μL aliquot of a fresh 2% UA solution was placed on the grid and left for 30 s, and excess UA solution was blotted with another clean filter paper. Air-dried samples were visualized with an FEI 200 kV Titan Themis STEM.

MALDI-TOF Mass Spectrometry Analysis. To carry out the MALDI-TOF mass spectrometry analysis, sinapinic acid (SA, 3,5-dimethoxy-4-hydroxy-cinnamic acid) was used as a matrix to absorb the laser energy and facilitate the ionization of the analyte molecules. The exosome sample was mixed with the matrix solution, and a small aliquot was deposited onto a MALDI target plate. The sample was then allowed to dry, forming a thin crystalline matrix layer with embedded exosome analytes. The target plate was then placed inside the MALDI-TOF mass spectrometer. A laser beam was focused on the sample spot, causing the matrix to absorb the laser energy and desorb and ionize the exosome analytes. This generated positively charged ions from the exosome molecules. The generated ions were then separated based on their mass-to-charge ratio (m/z) as they traveled through a flight tube.

ICV Injection of Modified Exosomes (Rho-BR-EVs). ICV injection is a method for administering medications or other substances directly into the CSF, allowing the fluid to circulate in the whole brain. ICV injection was performed as described in our previous publication.[26] In brief, SD rats were anesthetized with 5% isoflurane and maintained at 2.5% throughout the surgery. The rats were placed stereotaxically over the heating device, and their rectal temperature was maintained at approximately 37 °C. The cranium was exposed by incising the scalp over the sagittal suture between the eyes and ears and removing the periosteum. The stereotaxic apparatus was adjusted to align the bregma and lambda. A right hole was drilled through the cranium at the coordinates of the lateral ventricles.

The lateral ventricles had the following coordinates: 0.8 mm caudal to bregma, 1.6 mm in the mediolateral axis, and −3.6 mm in the dorsoventral axis. Using an UltraMicroPump 3 (World Precision Instruments), 5.5 μg of Rho-BR-EVs were injected into the lateral ventricle at a 1 μL/min rate. 24 h after ICV administration, the rats were perfused with ice-cold PBS and 4% paraformaldehyde (PFA). The rat brains were extracted, fixed overnight in a 4% PFA solution, and subjected to 30% sucrose in filtered PBS until the tissue sank. The brains were then embedded in the O.C.T. compound (Sakura Finetek) and cryo-sectioned into 15 μm thick coronal sections for fluorescence immunostaining as described below.

Immunofluorescence Staining. Immunostaining was performed as described in our previous publication,[27] with some modifications. Brain sections containing the cortex or hippocampus were washed in PBS 3 times for 10 min each and then incubated with 5% horse serum for 30 min. The sections were then incubated with the rabbit anti-NeuN antibody (Cell signaling, 1:300 dilution), rabbit anti-GFAP antibody (Abcam, 1:500 dilution), or rabbit anti-IBA1 antibody (Fujifilm Wako, 1:500 dilution) in PBS containing 0.5% Triton X-100 and 5% horse serum for 48 h at 4 °C. Afterward, brain sections were washed with PBS thrice for 10 min each. Brain sections were then incubated with the secondary antibody Alexa Fluor 488 donkey antirabbit IgG at room temperature for 1 h. The immunoreactivity of NeuN, GFAP, and IBA1, as well as the fluorescence of Rho-BR-EVs, was observed under a confocal microscope, and images were taken.

AUTHOR INFORMATION

Corresponding Authors

Zhiying Shan − *Department of Kinesiology and Integrative Physiology and Health Research Institute, Michigan Technological University, Houghton, Michigan 49931, United States;* orcid.org/0000-0002-9763-205X; Email: zhiyings@mtu.edu

Lanrong Bi − *Department of Chemistry, Michigan Technological University, Houghton, Michigan 49931, United States; Health Research Institute, Michigan Technological University, Houghton, Michigan 49931, United States;* orcid.org/0000-0001-6624-8314; Email: lanrong@mtu.edu

Authors

Xin Yan − *Department of Chemistry, Michigan Technological University, Houghton, Michigan 49931, United States; Health Research Institute, Michigan Technological University, Houghton, Michigan 49931, United States*

Xinqian Chen − *Department of Kinesiology and Integrative Physiology and Health Research Institute, Michigan Technological University, Houghton, Michigan 49931, United States*

Complete contact information is available at: https://pubs.acs.org/10.1021/acsomega.3c06617

Author Contributions

‖X.Y. and X.C. contributed equally.

Notes

The authors declare no competing financial interest.

ACKNOWLEDGMENTS

This project is partially supported by AHA 1807047 (Bi), NIHR15HL150703 (Shan), and NIHR01HL163159 (Shan). The authors express gratitude to Dr. Richard Koubek for fostering a supportive work environment for these ongoing projects.

https://doi.org/10.1021/acsomega.3c06617
ACS Omega 2023, 8, 48984−48993

REFERENCES

(1) Carey, A.; Fossati, S. Hypertension and hyperhomocysteinemia as modifiable risk factors for Alzheimer's disease and dementia: New evidence, potential therapeutic strategies, and biomarkers. *Alzheimer's Dementia* **2023**, *19* (2), 671−695.

(2) Zhang, W.; Mehta, A.; Tong, Z.; Esser, L.; Voelcker, N. H. Development of Polymeric Nanoparticles for Blood-Brain Barrier Transfer-Strategies and Challenges. *Adv. Sci.* **2021**, *8* (10), No. 2003937.

(3) Tomaszewski, W.; Sanchez-Perez, L.; Gajewski, T. F.; Sampson, J. H. Brain Tumor Microenvironment and Host State: Implications for Immunotherapy. *Clin. Cancer Res.* **2019**, *25* (14), 4202−4210.

(4) Kerwin, D.; Abdelnour, C.; Caramelli, P.; Ogunniyi, A.; Shi, J.; Zetterberg, H.; Traber, M. Alzheimer's disease diagnosis and management: Perspectives from around the world. *Alzheimers Dementia* **2022**, *14* (1), No. e12334.

(5) Mantle, D.; Hargreaves, I. P. Mitochondrial Dysfunction and Neurodegenerative Disorders: Role of Nutritional Supplementation. *Int. J. Mol. Sci.* **2022**, *23* (20), No. 12603.

(6) Lu, R. O.; Ho, W. S. Mitochondrial Dysfunction, Macrophage, and Microglia in Brain Cancer. *Front. Cell Dev. Biol.* **2021**, *8*, No. 620788.

(7) Falabella, M.; Vernon, H. J.; Hanna, M. G.; Claypool, S. M.; Pitceathly, R. D. S. Cardiolipin, Mitochondria, and Neurological Disease. *Trends Endocrinol. Metab.* **2021**, *32* (4), 224−237.

(8) Manevski, M.; Devadoss, D.; Castro, R.; Delatorre, L.; Yndart, A.; Jayant, R. D.; Nair, M.; Chand, H. S. Development and Challenges of Nanotherapeutic Formulations for Targeting Mitochondrial Cell Death Pathways in Lung and Brain Degenerative Diseases. *Crit Rev. Biomed. Eng.* **2020**, *48* (3), 137−152.

(9) Tang, B. L. Glucose, glycolysis, and neurodegenerative diseases. *J. Cell. Physiol.* **2020**, *235* (11), 7653−7662.

(10) Liu, Y.; Shi, Y. Mitochondria as a target in cancer treatment. *MedComm* **2020**, *1* (2), 129−139.

(11) Shekh, R.; Ahmad, A.; Tiwari, R. K.; Saeed, M.; Shukla, R.; Al-Thubiani, W. S.; Ansari, I. A.; Ashfaque, M.; Bajpai, P. High therapeutic efficacy of 5-Fluorouracil-loaded exosomes against colon cancer cells. *Chem. Biol. Drug Des.* **2023**, *101* (4), 962−976.

(12) Liu, S.; Fan, M.; Xu, J. X.; Yang, L. J.; Qi, C. C.; Xia, Q. R.; Ge, J. F. Exosomes derived from bone-marrow mesenchymal stem cells alleviate cognitive decline in AD-like mice by improving BDNF-related neuropathology. *J. Neuroinflammation* **2022**, *19* (1), No. 35.

(13) Li, J.; Li, J.; Peng, Y.; Du, Y.; Yang, Z.; Qi, X. Dendritic cell derived exosomes loaded neoantigens for personalized cancer immunotherapies. *J. Controlled Release* **2023**, *353*, 423−433.

(14) Han, Z.; Peng, C.; Yi, J.; Wang, Y.; Liu, Q.; Yang, Y.; Long, S.; Qiao, L.; Shen, Y. Matrix-assisted laser desorption ionization mass spectrometry profiling of plasma exosomes evaluates osteosarcoma metastasis. *iScience* **2021**, *24* (8), No. 102906.

(15) Zeng, Q.; Li, T.; Cash, B.; Li, S.; Xie, F.; Wang, Q. Chemoselective derivatization of a bionanoparticle by click reaction and ATRP reaction. *Chem. Commun.* **2007**, No. 14, 1453−1455.

(16) Smyth, T.; Petrova, K.; Payton, N. M.; Persaud, I.; Redzic, J. S.; Graner, M. W.; Smith-Jones, P.; Anchordoquy, T. J. Surface functionalization of exosomes using click chemistry. *Bioconjugate Chem.* **2014**, *25* (10), 1777−1784.

(17) Yapici, N. B.; Mandalapu, S.; Gibson, K. M.; Bi, L. Targeted fluorescent probes for detection of oxidative stress in the mitochondria. *Bioorg. Med. Chem. Lett.* **2015**, *25* (17), 3476−3480.

(18) Yapici, N. B.; Bi, Y.; Li, P.; Chen, X.; Yan, X.; Mandalapu, S. R.; Faucett, M.; Jockusch, S.; Ju, J.; Gibson, K. M.; Pavan, W. J.; Bi, L. Highly stable and sensitive fluorescent probes (LysoProbes) for lysosomal labeling and tracking. *Sci. Rep.* **2015**, *5*, No. 8576.

(19) Yapici, N. B.; Gao, X.; Yan, X.; Hou, S.; Jockusch, S.; Lesniak, L.; Gibson, K. M.; Bi, L. Novel Dual-Organelle-Targeting Probe (RCPP) for Simultaneous Measurement of Organellar Acidity and Alkalinity in Living Cells. *ACS Omega* **2021**, *6* (47), 31447−31456.

(20) Chen, X.; Bi, Y.; Wang, T.; Li, P.; Yan, X.; Hou, S.; Bammert, C. E.; Ju, J.; Gibson, K. M.; Pavan, W. J.; Bi, L. Lysosomal targeting with stable and sensitive fluorescent probes (Superior LysoProbes): applications for lysosome labeling and tracking during apoptosis. *Sci. Rep.* **2015**, *5*, No. 9004.

(21) Yapici, N. B.; Mandalapu, S. R.; Chew, T. L.; Khuon, S.; Bi, L. Determination of intracellular pH using sensitive, clickable fluorescent probes. *Bioorg. Med. Chem. Lett.* **2012**, *22* (7), 2440−2443.

(22) Gao, H.; Bigalke, J.; Jiang, E.; Fan, Y.; Chen, B.; Chen, Q. H.; Shan, Z. TNFα Triggers an Augmented Inflammatory Response in Brain Neurons from Dahl Salt-Sensitive Rats Compared with Normal Sprague Dawley Rats. *Cell. Mol. Neurobiol.* **2022**, *42* (6), 1787−1800.

(23) Crescitelli, R.; Lässer, C.; Lötvall, J. Isolation and characterization of extracellular vesicle subpopulations from tissues. *Nat. Protoc.* **2021**, *16* (3), 1548−1580.

(24) Vella, L. J.; Scicluna, B. J.; Cheng, L.; Bawden, E. G.; Masters, C. L.; Ang, C. S.; Willamson, N.; McLean, C.; Barnham, K. J.; Hill, A. F. A rigorous method to enrich for exosomes from brain tissue. *J. Extracell. Vesicles* **2017**, *6* (1), No. 1348885.

(25) Shan, Z.; Cuadra, A. E.; Sumners, C.; Raizada, M. K. Characterization of a functional (pro)renin receptor in rat brain neurons. *Exp. Physiol.* **2008**, *93* (5), 701−708.

(26) Jiang, E.; Chapp, A. D.; Fan, Y.; Larson, R. A.; Hahka, T.; Huber, M. J.; Yan, J.; Chen, Q. H.; Shan, Z. Expression of Proinflammatory Cytokines Is Upregulated in the Hypothalamic Paraventricular Nucleus of Dahl Salt-Sensitive Hypertensive Rats. *Front. Physiol.* **2018**, *9*, No. 104.

(27) Huber, M. J.; Basu, R.; Cecchettini, C.; Cuadra, A. E.; Chen, Q. H.; Shan, Z. Activation of the (pro)renin receptor in the paraventricular nucleus increases sympathetic outflow in anesthetized rats. *Am. J. Physiol.-Heart Circ. Physiol.* **2015**, *309* (5), H880−H887.

https://doi.org/10.1021/acsomega.3c06617
ACS Omega 2023, 8, 48984−48993